UHPFRC DIRECT SHEAR CHARACTERIZATION APPLIED TO WEB-FLANGE SHEAR DESIGN OF T-SHAPED GIRDERS

Amaury Herrera (1), Florent Baby (2), Pierre Marchand (3) and François Toutlemonde (3)

(1) Cerema, DTerMed, Aix-en-Provence, France

(2) Direction de l'environnement, de l'aménagement et du logement, La Réunion, France

(3) Paris-Est University / IFSTTAR, Materials & Structures Dep^{t}, Marne-la-Vallée, France

Abstract

Shear verification may turn out as critical in a number of ultra-high performance fibre-reinforced concrete (UHPFRC) structures, e.g. at the web to flange junction in a T-shaped beam. Present design provisions have been compared with a comprehensive experimental campaign, whose analysis takes into account the effective local response of the fibre-reinforced material. The investigation comprises direct shear tests on notched prisms made of 3 UHPFRC mixes with different fibre contents both on moulded specimens and sawn ones from representative junction zones. Combined with the standard characterization tests and limit analysis models, these results have been used to analyse the experimental response of 5.60 meter long T-shaped beams, specially designed to exhibit a longitudinal shear failure mode at the web to flange junction. The results evidence the contribution of UHPFRC under shear and tension in the different situations of fibre distribution and orientation.

Résumé

La vérification de la résistance au cisaillement peut s'avérer critique dans le dimensionnement de nombreuses structures en béton fibré à ultra-hautes performances (BFUP), par exemple à la jonction entre âme et table d'une poutre en T. Les dispositions de conception actuelles ont été confrontées à une étude expérimentale approfondie dont l'interprétation prend en compte le comportement local effectif du matériau fibré. L'investigation comprend des essais de cisaillement pur sur prismes entaillés constitués de 3 BFUP comprenant différents taux de fibres, à la fois sur éprouvettes moulées et prélevées par sciage dans des zones représentatives des jonctions. Associés aux essais de caractérisation normalisés et à des modèles d'analyse limite, ces résultats ont été utilisés pour interpréter le comportement expérimental de poutres en T de 5,60 mètres de longueur, spécifiquement dimensionnées pour mettre en évidence un mode de rupture en cisaillement longitudinal à la jonction de l'âme et de la table. Les résultats mettent en évidence la contribution du BFUP cisaillé ou tendu dans les différentes configurations d'orientation et de distribution des fibres.

1. INTRODUCTION

Shear verification of ultra-high performance fibre-reinforced concrete (UHPFRC) structures especially at junctions may turn out as critical in a number of structures. This may concern bridge structures or building components like bulb-Tee girders, ribbed decks, shells connected to stiffeners, etc. Safe provisions have been adopted in the presently enforced French standard for the design of UHPFRC structures [1], excluding combination of the tensile and shear capacities of the UHPFRC material in the same part of a cross-section. This may however result in unnecessary addition of steel reinforcement, or thickening of flanges or webs, which counteract the search for lightness and material savings and may even jeopardize the favourable fibre orientation. It was thus deemed opportune to develop improved shear design verification methods of such zones, taking into account as reliably as possible the material and fibre contributions to possibly dispense with secondary reinforcement. Due to limited available data addressing shear behaviour of UHPFRC, an experimental program was launched in order to investigate the shear capacity of this class of materials, in relation to both the enhanced matrix tensile / shear strength and the fibre contribution. The obtained material characteristics were related to the results of dedicated bending tests of pre-stressed bulb-Tee-shaped beams, whose capacity was intended to be critically determined by the shear resistance of the web to flange junction.

2. DIRECT SHEAR TESTS

The configuration of direct shear tests was selected to create a single shear plane in the tested specimen and to limit complex shapes which would have disturbed fibre isotropic distribution for the moulded specimens. A setup derived from [2] was designed, using high quality steel to avoid yielding of the rolls due to concentrated pressure (Fig. 1). The test can be applied to moulded or sawn prisms. The actuator is displacement-controlled and a notch is provided along all the specimen sides to promote failure in the notched plane. Two specimens have been tested for each mix. Opening and shear displacement along the plane submitted to direct shear were measured on both sides. The shear stress is obtained as V=7×P/8 divided by the net cross-section area of the notched prism. Details can be found in [3].

Three UHPFRC mixes representative of currently available materials, of 200 to 230 MPa-average compressive strength, with fibre contents ranging from 1.0 to 3.0 %, and maximum nominal aggregate sizes ranging from 0.6 to 6.0 mm (Table 1), were characterized. Besides the direct shear tests on sawn prisms, bending tensile tests according to the French standard method for determination of the tensile constitutive design curve of the material [4] and compressive tests on cylinders, including measurement of Young’s modulus, compressive strength and Poisson’s ratio, were carried out.

Table 1: Characteristics of the UHPFRC mixes

Mix	Fiber content (%)	Max. Aggregate Size (mm)	Fiber length (mm)
A	1	0.8	14
B	3	0.8	14
C	2.5	5	20

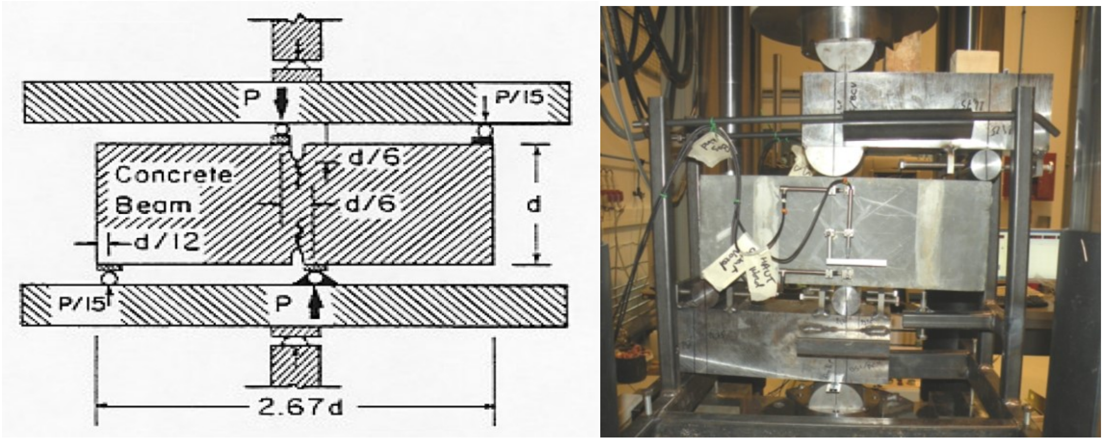

Figure 1: Direct shear test setup, derived from [2]. d = 185 mm in the present tests.

2.1 Intrinsic shear strength

Results obtained on moulded prisms are displayed on Fig. 2 and in Table 2. The maximum force is obtained after a significant non-linear phase of the response, typically corresponding to contribution of the fibres to resist shear after cracking (dowel + group effects).

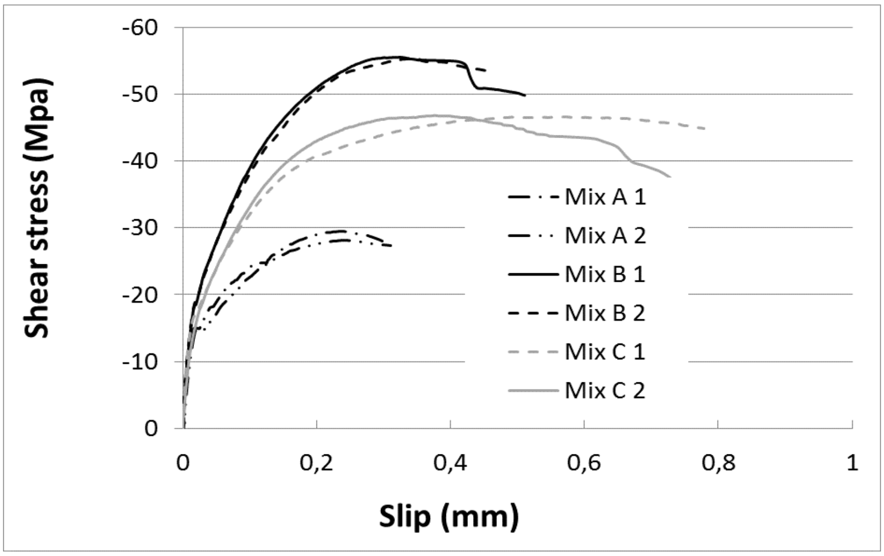

Figure 2: Test results: Shear stress vs. average slip for each specimen

Table 2: Main figures associated to the direct shear tests of moulded specimens

Mix	A		B		C	
Specimen number	1	2	1	2	1	2
Limit of linearity (MPa)	15.0	14.8	18.2	18.8	16.6	10.2*
Maximum shear stress (MPa)	29.5	28.2	55.5	55.2	46.5	46.8
Average crack opening at peak stress (mm)	0.29	0.33	0.3	0.39	0.54	0.47
Maximum crack opening at failure (mm)	0.37	0.47	0.47	0.47	0.75	0.80
Maximum slip at failure (mm)	0.29	0.31	0.50	0.46	0.77	0.75

* local loss of linearity for only one of the sensors

Maximum slip and crack opening correspond to the physical failure of the specimens in two pieces. From post-failure examination of the specimens, it turns out that a significant part of the fibres were broken along the failure surface, which explains a relatively low ductility, as compared to the tensile behaviour of these UHPFRC mixes (especially B and C). The maximum shear stress capacity evidenced from these tests is however significantly higher than the documented results from the literature [5]. As a rough estimate, the ultimate shear stress equals 3.6 times the tensile strength determined following [4]. It also exhibits a linear dependency on the fibre content (Fig. 3), which can be reasonably compared to the linear dependency of the shear capacity of a reinforced concrete joint, as given in most of design code provisions (e.g., clause 6.2.5 of [1] or [6]).

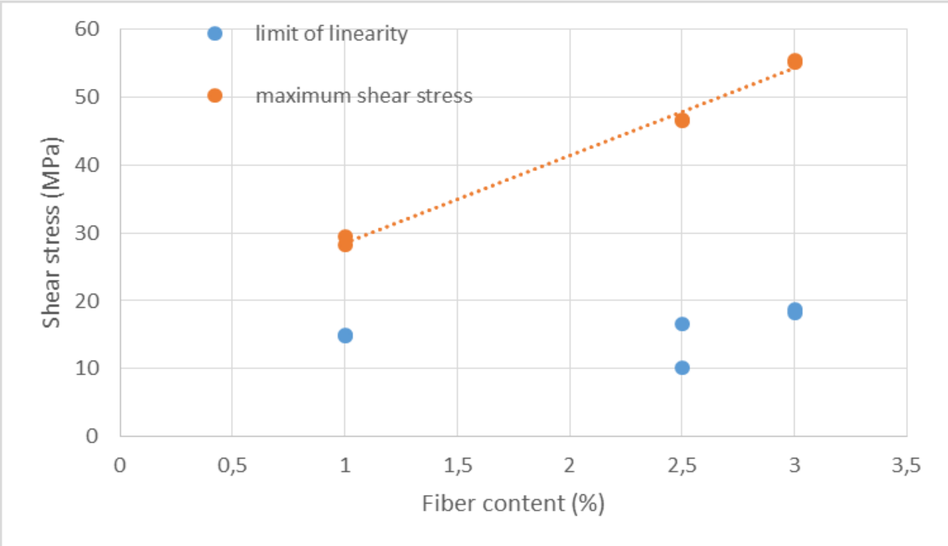

Figure 3: Shear stress capacity and limit of linearity vs. fiber content (moulded specimens)

2.2 Characterization of sawn specimens

It was suspected that the results obtained from the moulded prisms correspond to a very favourable situation with respect to isotropic fibre distribution and efficiency. In a junction however, especially when no gusset is provided, orientation of the fibres may be disturbed due to the conflict between the different two-dimensional orientation of the fibres promoted in each of the thin planes or shell elements converging to the junction, depending on the UHPFRC placement method and on the mix viscosity. Therefore, it was deemed as useful to characterise also the shear capacity of UHPFRC as placed.

Prisms with a cross-sectional area of 3.5 × 15 cm² (very similar to the 4.0 × 15 cm² - net cross section of moulded specimens) were sawn in the Tee-shaped beams described hereafter. Main results are displayed in Table 3. The limit of linearity is reduced by around 20 %, which may be partly due to the different casting and curing conditions. More significantly, the maximum shear stress is reduced by a factor of 2 to 3, still being higher than the tensile strength (as would be the theoretical situation with a brittle material). As a clear consequence, control of the fibre orientation and optimization of the casting process in the junctions is a first (and maybe sometimes hardly achieved) condition for avoiding extra-thickness or additional passive reinforcement in these zones.

Table 3: Main figures associated to the direct shear tests of sawn specimens

Mix	A		B		C	
Specimen number	A1	A2	B1	B2	C1	C2
Limit of linearity (MPa)	11.9	12.1	15.5	10.9	14.3	13.3
Maximum shear stress (MPa)	12.2	12.9	25.2	21.7	17.8	14.7
Average crack opening at peak stress (mm)	0.20	0.28	0.28	0.32	0.41	0.40

3. FAILURE TESTS OF T-SHAPED BEAMS

Tee-shaped beams represent the typical local situation of a junction between planes or slightly curved shells. Most critical concomitant internal forces are represented by the axial force within the web of the beam, longitudinal bending of the beam, and possibly transverse bending (generally corresponding to forces applied on the table). Horizontal and vertical shear forces are induced along the junction, which may be critical in case of a very thin table. In this first stage, only longitudinal bending was applied in a centred four-point bending scheme.

3.1 Preliminary design: specimen, test setup and monitoring

The specimen, whose dimensions are shown Fig. 4, was sized in order to promote horizontal shear failure along the junction between the table and the 110 mm-thick web of the beam. Thus a total of 10 pre-stressing tendons were located in the bulb of the beam to increase bending and vertical shear resistance, and the table was only 50 mm-thick. As compared to usual UHPFRC components, the web was relatively thick and the sharp re-entrant corner was under-optimal. The shear span (1.40 m) roughly equals 3 times the beam depth so that assumptions for the development of a possible truss mechanism are valid. Based on preliminary material data, shear failure within the table should be observed as the dominant failure mode after the development of diagonal cracking due to vertical shear within the web. The beams were fabricated in representative industrial conditions. Concrete was placed from above the web and it was avoided with the successive batches to keep a free surface of cast concrete as a temporary cold joint along the bottom of the table. However, the top of the web intersecting the table may have been a zone of fibers diffusion towards the wings of the table as well as a zone of longitudinal movement of the material. Prestressing tendons were equipped with strain gauges, and temperature was monitored, so that prestressing losses have been estimated rather accurately and initial stresses within the specimen can be reliably evaluated.

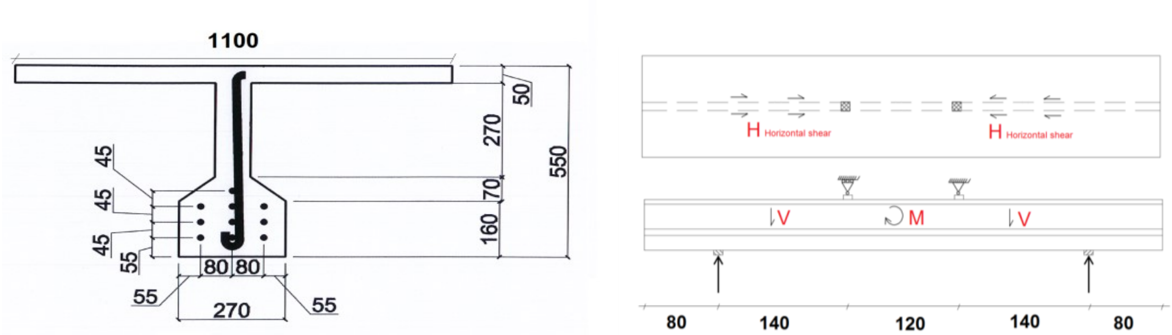

Figure 4: Specimens dimensions (left, in mm) and loading scheme (right, in cm)

As illustrated Fig. 5, the load was applied from the bottom ends to keep the upper surface free for easier observation and for possible concomitant loading, applying transverse bending. Control of the load applied was performed in series with all actuators and at reaction points. The beam deflection was monitored at 13 regularly-spaced locations. Extensometers were fixed to the vertical sides of the web at 45°, to detect and monitor the effects of vertical shear (diagonal tension). The top surface was equipped in the table wings with sensors at 120° to measure the strains and their orientation. Perpendicular extensometers were fixed along the junction in the shear span to survey the possible shear-slip mechanism along the junction. Finally, one side of the top surface outside of the constant moment zone was monitored with successive pictures processed by digital image correlation (DIC). The beams were subjected to several successive loading cycles of increasing intensity in the elastic domain, and then loaded up to failure at a quasi-static rate.

Figure 5: Loading setup with a T-shaped beam specimen to be tested.

3.2 Cracking process and failure modes

Two main cracking modes were observed for all specimens, in relation to vertical and horizontal shear, respectively (Fig. 6). Fine distributed diagonal cracks were first observed due to vertical shear. Their occurrence had been predicted for a total vertical load from 960 to 1160 kN depending on the UHPFRC-mix tensile limit of elasticity, yet they were visible for a much lower load (from 450 to 750 kN), possibly be due to restrained shrinkage effects [7].

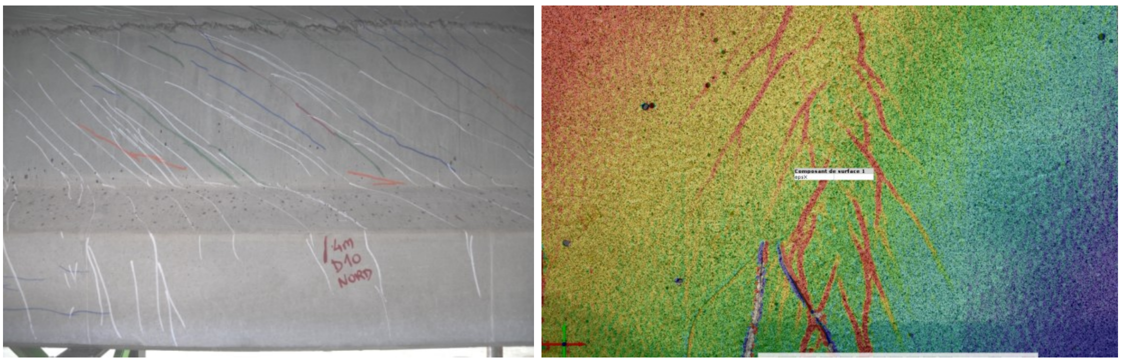

Figure 6: Local cracking modes: diagonal tension due to vertical shear (left), fish-bone crack pattern evidenced using DIC, due to horizontal shear (right).

Occurrence of fish-bone cracks visible from the top of the beam deck, on both sides of the junction with the web, was observed at a vertical load of about 1000 kN for beams made of mix A, 1200 to 1600 kN for beams made of mix B, and 1700 kN for beams made of mix C. These values are not directly related to the UHPFRC mix shear strength. Moreover, similarly to vertical shear cracks, these cracks did not fully develop into a kinematic mechanism leading to a failure scheme corresponding to a truss mechanism which would have corresponded to the yield lines mechanism assumed for design, e.g. in clause 6.2.4 of Eurocode 2 [6]. On the contrary, the increasing horizontal shear force led to the propagation of a vertical crack along the junction, which is made clearly visible from DIC for the beams made of UHPFRC mix A (Fig. 7).

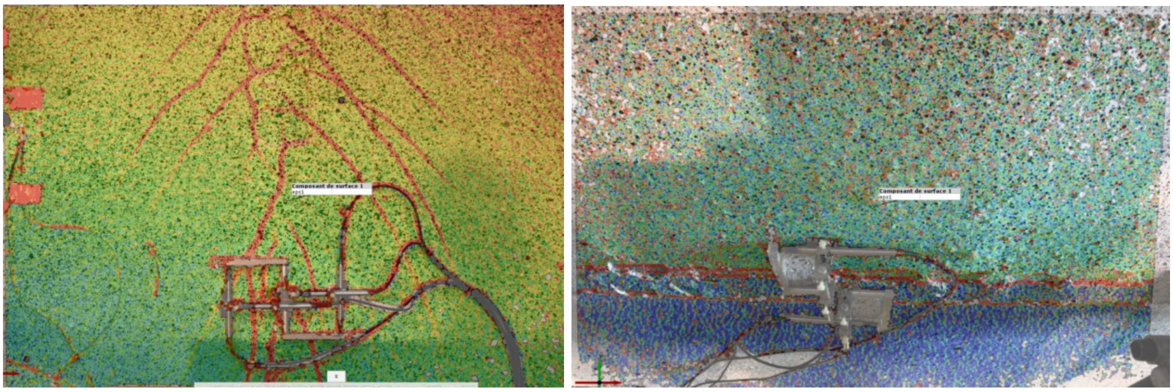

Figure 7: Horizontal shear, from fish-bone cracking (left) to shear-slip failure (right).

Figure 8: Horizontal shear, full development of the shear-slip mechanism (beams Aa, Ab, Ba).

Figure 9: Major cracks (with link failure) developed due to vertical shear (beam Ba).

This vertical crack fully developed in a shear-slip failure mechanisms for beams made of UHPFRC mix A and for one of the beams made of UHPFRC mix B (Fig. 8), with separation of one or both of the wings of the beam deck from the web. For this beam made of UHPFRC mix B however, major vertical shear cracks developed as a sign of more complex failure modes interaction (Fig. 9). For the other beam made of UHPFRC mix B, as well as for the beams made of UHPFRC mix C, bending failure either due to tendons yielding or to UHPFRC crushing in the constant bending moment zone occurred before the full development of the vertical crack of the junction (Fig. 10).

Figure 10: Bending failure mode: UHPFRC crushing (left, beam Ca) vs. tendons failure (right, beams Bb, Cb)

3.3 Failure loads and limit analysis

The global response of the beams is displayed on Fig. 11 in an applied load vs. mid-span deflection diagram. As evidenced from this figure, strong decrease in rigidity for beams Aa and Ab made of UHPFRC mix A occurs for a load close to 800 kN, which corresponds to initiation of the failure crack at the junction. Failure occurs for these beams at 1100 to 1200 kN. For beams Ba and Bb made of UHPFRC mix B, the significant change in rigidity and initiation of non-linear behaviour occurs for an applied load close to 1380 kN which also corresponds to visible initiation of the vertical crack at the junction. Failure however occurs at 1880 to 1950 kN, the development of the junction slip failure being overtaken by the other mechanisms. Similarly for beams Ca and Cb, the significant change in rigidity and initiation of non-linear behaviour occurs for an applied load close to 1200 kN, and failure occurs due to bending at an applied load of 1900 to 1950 kN, the development of the junction slip failure being overtaken by this latter mechanism.

The global beams response has been satisfactorily predicted using an advanced model based on modified strength of materials, assuming superposition of strains induced by longitudinal bending, longitudinal shear and transverse shear if relevant, and accounting for stiffness decrease in a confined zone corresponding to controlled multiple cracking development by using the MCFT theory [8] adapted to UHPFRC, following assumptions detailed in [9] and [3]. This means that local tensile damage and simple assumptions for describing biaxial effects may be deemed as sufficient for predicting the global response of structures like the T-beams considered. It has also been shown however that the failure loads and modes could not be satisfactorily predicted from an objective criterion based on an ultimate tensile strain, which confirms a difficulty already emphasized in [10] (and [1], annex V). In fact, experimental results detailed hereafter would correspond to an ultimate strain close to 3 mm/m in the case of mix A and 9 mm/m in the case of mixes B and C, without possible *a priori* justification. Namely, the standard UHPFRC characterization based on bending tests of thin plates [4] is not representative of multiple cracking imposed by the boundary conditions. For mix A, a stress-crack opening curve is derived with no evidence of the ultimate tensile strain; for mixes B and C the ultimate strain of the mean curve is about 8 to 9 mm/m while it is about 3 mm/m for the characteristic curve.

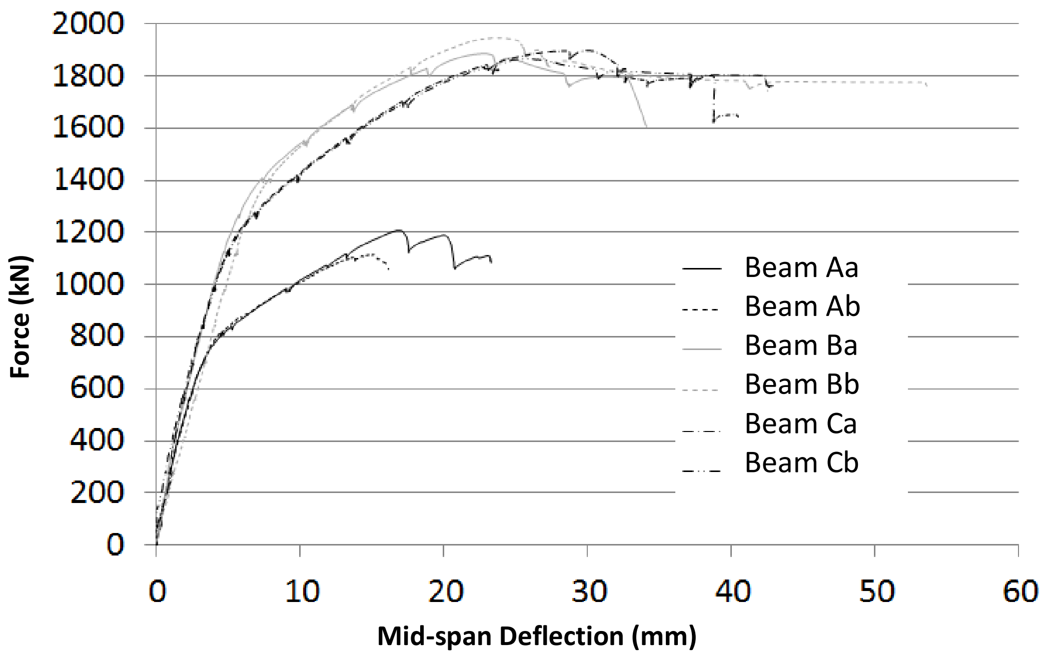

Figure 11: Global beam response in a load vs. mid-span deflection diagram

It is thus necessary to check in detail the succession of yielding / failure modes as evidenced from the experience to possibly determine the limit analysis mechanisms that could help predicting the effective capacity of the tested structures, while only the prediction of the beams capacity associated to bending mechanisms appears as reliable enough. Especially for beams Aa, Ab and Ba where the slip failure mechanism along the junction has been evidenced, it would be desirable to correlate the failure load to the ultimate shear stress identified from sawn specimens (Table 3).

As a possible upper bound approach, a horizontal shear-resisting truss mechanism could be assumed. The ultimate shear-resisting length at the junction has to be counterbalanced by a compressed strut at 45° within the deck. From geometrical considerations, this length thus corresponds to one wing width minus the deck thickness, namely about 45 cm with the dimensions of the tested beams. Ultimate shear of mix A (12 MPa) would correspond to a maximum failure load of beams close to 1100 kN, while ultimate shear of mix B (22 MPa) would correspond to a maximum failure load of beams close to 1980 kN. For these cases the order of magnitude would be reasonable. It is unclear however why this simplistic quantitative rule does not satisfactorily apply to beams made of mix C. Further work is thus needed to better address a satisfactory shear design procedure based on effective evidenced mechanisms.

4. CONCLUSION

For a better quantitative understanding of shear resistance, which may turn out as critical for design of a number of UHPFRC structures, e.g. at the web to flange junction in a T-shaped beam, a comprehensive experimental campaign has been carried out. The investigation has comprised direct shear tests on notched prisms made of 3 UHPFRC mixes with different fibre contents both on moulded specimens and sawn ones from representative junction zones. Relatively high values of UHPFRC intrinsic shear capacity have been obtained in case of an optimized casting process with well distributed and oriented fibres, with a meaningful correlation with tensile strength and fibre content. Combined with the standard characterization tests and limit analysis models, these results have been used to analyse the experimental response of six 5.60 meter long T-shaped beams, specially designed to exhibit a longitudinal shear failure mode at the web to flange junction. The UHPFRC shear capacity appears as highly depending on local fibre distribution and further research is needed to validate operational limit analysis methods for a predictive assessment of the structures capacity when determined by the shear failure of the junction.

ACKNOWLEDGEMENTS

This experimental program has been sponsored by LafargeHolcim, Eiffage and Vicat. Sébastien Bernardi, Alain Simon and Florian Chalencon are gratefully acknowledged, as well as Yves Brugeaud for having organized the beams fabrication. Moreover, the authors are pleased to thank the technicians of IFSTTAR Structures Laboratory who contributed to the tests, especially Lénaïc Baron, Marc Estivin, Gonzague Six and Jean-Claude Renaud.

REFERENCES

[1] AFNOR (2016) NF P 18-710, National addition to Eurocode 2 — Design of concrete structures: specific rules for Ultra-High Performance Fibre-Reinforced Concrete (UHPFRC).

[2] Bažant, Z. P., & Pfeiffer, P. A. (1986) Shear fracture tests of concrete, *Materials and Structures*, Vol. **19** (2), No 110, pp. 111-121.

[3] Herrera A. (2017), Fonctionnement des jonctions âmes-membrures en Béton Fibré à Ultra-Hautes Performances (BFUP), Ph.D. Thesis, Paris-Est Univ.-IFSTTAR, France, 441 pages.

[4] AFNOR (2016) NF P 18-470, Ultra-high Performance fibre-reinforced concrete: Specification, performance, production and conformity.

[5] Crane, C. K. (2010) Shear and shear friction of ultra-high performance concrete bridge girders, PhD Thesis, Georgia Institute of Technology.

[6] AFNOR (2005) NF EN 1992-1-1, Eurocode 2. Design of concrete structures. Part 1-1 : General rules and rules for buildings.

[7] Sato R., Kawakane H., Kawamoto T., Ushio R., Maruyama I. (2007) Shrinkage Effect on Shear Strength of Reinforced, High Strength Concrete Beams, ACI SP-246, pp. 261-278.

[8] Vecchio F., Collins M. P. (1986) The modified compression field theory for reinforced concrete elements subjected to shear, *ACI Materials Journal*, vol. 83 pp. 219-231.

[9] Baby, F. (2012) Contribution à l'identification et la prise en compte du comportement en traction des BFUP à l'échelle de la structure, Ph.D. Thesis, Paris-Est Univ.-IFSTTAR, France, 522 pages.

[10] Sorelli L., Davila R., De Jesus M., Ulm F.-J., Toutlemonde F. (2007) Optimal design of UHPC highway bridges based on crack criteria, CONSEC'07, pp. 1085-1092.